Combinatorial Selection, Inhibition, and Antiviral Activity of DNA Thioaptamers Targeting the RNase H Domain of HIV-1 Reverse Transcriptase†

Anoma Somasunderam,‡ Monique R. Ferguson,§ Daniel R. Rojo,§ Varatharasa Thiviyanathan,‡ Xin Li,‡ William A. O'Brien,§ and David G. Gorenstein*,‡

Department of Human Biological Chemistry and Genetics and Division of Infectious Diseases, Department of Internal Medicine, University of Texas Medical Branch, Galveston, Texas 77555

Received April 18, 2005; Revised Manuscript Received June 4, 2005

ABSTRACT: Despite the key role played by the RNase H of human immunodeficiency virus-1 reverse transcriptase (HIV-1 RT) in viral proliferation, only a few inhibitors of RNase H have been reported. Using in vitro combinatorial selection methods and the RNase H domain of the HIV RT, we have selected double-stranded DNA thioaptamers (aptamers with selected thiophosphate backbone substitutions) that inhibit RNase H activity and viral replication. The selected thioaptamer sequences had a very high proportion of G residues. The consensus sequence for the selected thioaptamers showed G clusters separated by single residues at the 5′-end of the sequence. Gel electrophoresis mobility shift assays and nuclear magnetic resonance spectroscopy showed that the selected thioaptamer binds to the isolated RNase H domain, but did not bind to a structurally similar RNase H from *Escherichia coli*. The lead thioaptamer, R12-2, showed specific binding to HIV-1 RT with a binding constant (K_d) of 70 nM. The thioaptamer inhibited the RNase H activity of intact HIV-1 RT. In cell culture, transfection of thioaptamer R12-2 (0.5 μg/mL) markedly inhibited viral production and exhibited a dose response of inhibition with R12-2 concentrations ranging from 0.03 to 2.0 μg/mL (IC_{50} < 100 nM). Inhibition was also seen across a wide range of virus inoculum, ranging from a multiplicity of infection (moi) of 0.0005 to 0.05, with a reduction of the level of virus production by more than 50% at high moi. Suppression of virus was comparable to that seen with AZT when moi ≤ 0.005.

Reverse transcription of viral genomic RNA into DNA, an essential step in the replication of human immunodeficiency virus type 1 (HIV-1)[1] and other retroviruses, is catalyzed by reverse transcriptase. The bifunctional HIV-1 RT is a heterodimer with 66 and 51 kDa subunits (*1*). Both subunits contain a DNA polymerase domain. The 66 kDa domain, p66, contains an RNase H domain in addition to the DNA polymerase domain. The DNA polymerase utilizes both RNA and DNA templates to accomplish viral genomic replication. RNase H catalyzes cleavage of the viral RNA strand from the DNA−RNA hybrid duplex, thereby releasing the viral DNA copy to ultimately integrate into the host cell's genome.

HIV infection progresses to AIDS at variable rates in virtually every infected individual over a period of several years in the absence of therapy. RT inhibitors were the first class of antiretroviral drugs approved and used to treat HIV infection. Although newer drugs targeting the HIV protease and, more recently, the envelope proteins have been approved for use, RT inhibitors remain an important component of combination therapy known as highly active antiretroviral therapy (HAART). Most commonly used HAART regimens typically include two or three RT inhibitors. The use of HAART, rather than less intensive antiretroviral regimens, has dramatically reduced the rates of progression to AIDS and has improved survival (*2*). Currently available RT inhibitors target the polymerase activity and are either nucleoside analogue drugs that bind at the polymerase active site or non-nucleoside inhibitors that bind to a different region of the HIV-1 RT. Therapeutic benefits can be markedly diminished by the emergence of drug resistant strains and by the potential toxicity of the approved antiretroviral drugs (*3*, *4*). Resistance to these drugs emerges rapidly because of the highly error-prone RT, and by the potential for recombination between different strains when cells are co-infected (*5*). Because of extensive cross-resistance within each drug class that reduces antiviral activity and clinical benefit of sequential HAART, there is an urgent need to develop new agents and treatment approaches to fight AIDS. This search for alternate targets and new agents has led to a new class of RT inhibitors known as oligonucleotide reverse transcriptase inhibitors (ONRTIs) (*6*, *7*).

ODNs are emerging as potential therapeutic agents that can be attractive alternatives for the chemical drugs (*8*, *9*). ODNs operate via different mechanisms, such as the

† This work was supported by grants from the NIAID/National Institutes of Health (U01-A1054827 and A127744 to D.G.G. and R21 AI058194-01A2 to M.R.F.) and the Welch Foundation (H-1296 to D.G.G.).

* To whom correspondence should be addressed: Department of HBC&G, 301 University Blvd., Galveston, TX 77555-1157. Phone: (409) 747-6800. Fax: (409) 747-6850. E-mail: david@nmr.utmb.edu.

‡ Department of Human Biological Chemistry and Genetics.

§ Division of Infectious Diseases, Department of Internal Medicine.

[1] Abbreviations: EMSA, electrophoretic mobility shift assay; HAART, highly active antiretroviral therapy; HIV-1, human immunodeficiency virus type 1; HSQC, heteronuclear single-quantum coherence; moi, multiplicity of infection; NMR, nuclear magnetic resonance; NOESY, nuclear Overhauser enhancement spectroscopy; ODN, oligonucleotide agents; RNase, ribonuclease; RT, reverse transcriptase.

10.1021/bi0507074 CCC: $30.25
Published on Web 07/08/2005

sequence-specific translational arrest of mRNA expression (antisense), RNA inhibition using specific short double-stranded RNA (siRNA), or binding to and inhibiting RT or other HIV proteins and cellular receptors (aptamers or decoys) (*10*−*12*). The antisense strategy, proposed for the potential treatment of several diseases, including AIDS and cancer (*13*), is based on the binding of ODNs to the mRNA by complementary base pairing. The decoy (or sense) strategy relies on selective binding of the ODNs, possibly selected as aptamers, to a nucleic acid binding protein. The decoy aptamer mimics the protein's natural ligand and, therefore, competes with it for complex formation with the protein. This association traps the protein in a nonfunctional complex. An advantage of aptamers over the antisense technology is that the aptamer ODNs do not have to overcome the thermodynamic penalty required for the unfolding of their own and the target's secondary and tertiary structures. RNA and DNA aptamers targeting several HIV proteins have been reported. This includes the inhibition of HIV-1 RT's polymerase (*14*, *15*) and RNase H activities (*16*, *17*), HIV-1 integrase function (*18*), and the capsid protein NCp7 (*19*, *20*).

Backbone modifications in ODNs are essential for increasing their resistance to digestion by cellular nucleases. Sulfur substitutions of phosphoric oxygens of the DNA backbone, as in monothiophosphate and dithiophosphate aptamers, often enhance their binding to proteins (*21*, *22*). One can also take advantage of the increased affinity of the ODNs generally associated with sulfur substitutions; however, complete substitution of the backbone could lead to nonspecific binding and therefore to a loss in specificity of the ODN to the target protein. Therefore, the number and position of sulfur substitutions in these thioaptamers need to be optimized to weaken binding to nontarget proteins while enhancing binding to the target protein.

Despite the key role played by HIV RT RNase H in viral proliferation, aptamers that specifically target this domain have not yet been reported. Although aptamers inhibiting RNase H activity have been reported, they were selected against the entire HIV RT. We have used the RNase H domain of HIV-1 RT in our selection process to select, by definition, thioaptamers that bind directly to RNase H. In this paper, we report the in vitro combinatorial selection of monothiophosphate-modified DNA thioaptamers that selectively bind to the RNase H domain of HIV-1 RT, inhibit RNase H activity, and exhibit antiretroviral activity.

MATERIALS AND METHODS

Materials. NTPs and HIV-1 RT were purchased from Amersham Bioscience (Piscataway, NJ). [^{3}H]UTP was purchased from NEN (Boston, MA). The chirally pure S_p isomer of dATP (αS) was obtained from Biolog Life Science Institute (Bremen, Germany). TOPO TA cloning kits were obtained from Invitrogen (Carlsbad, CA); the plasmid isolation kits were obtained from Qiagen (Foster City, CA), and AmpliTaq DNA polymerase and other PCR consumables were purchased from Applied Biosystems (Foster City, CA). The transfection agent Oligofectamine (OF) was purchased from Invitrogen.

Preparation of HIV-1 RNase H. We have constructed a new T7 RNA polymerase/IPTG-inducible plasmid whose insert encodes the 15 kDa RNase H domain of HIV-1 RT. The plasmid containing the coding region of HIV-1 RNase H (strain HXB2) was cloned into the pET30a(+) vector (Novagen), transformed and expressed in *Escherichia coli*, and purified as described previously (*23*). Both unlabeled and uniformly ^{15}N-labeled protein were purified to homogeneity after the overexpression in minimal medium or minimal medium containing $^{15}NH_4Cl$. This procedure yields excellent quantities of pure RNase H (ca. 20 mg/L in an *E. coli* expression system). Expression tests in rich, minimal, and ^{15}N-labeled minimal media provided the 15 kDa fragment (by SDS−PAGE). The authenticity of the protein was confirmed by N-terminal sequencing and NMR spectroscopy.

5'-ATGCTTCCACGAGCCTTTC---$(N)_{22}$---CTGCGAGGCGGTAGTCTATTC-3'

FIGURE 1: DNA library sequence. The random region is marked as N_{22}. The sequence has a 19-mer forward primer and a 21-mer reverse primer.

Synthesis of DNA Libraries. The chemically synthesized random combinatorial library is a 62-nucleotide single-strand DNA containing a 22-nucleotide random region flanked by 19- and 21-nucleotide PCR primer regions (Figure 1). The library was annealed with the reverse primer, subjected to the Klenow reaction for 5 h at 37 °C, and amplified by PCR using AmpliTaq DNA polymerase and a mixture of dATP(αS), dTTP, dCTP, and dGTP to give the thioaptamer-substituted library. Reaction conditions for the PCR amplifications were as follows: oligonucleotide library (40 nM), dATP(αS) (160 μM), mixture of dTTP, dCTP, and dGTP (80 μM each), $MgCl_2$ (2 mM), primer (400 nM each), and AmpliTaq DNA polymerase (1 unit) in a total volume of 100 μL. The PCR was run for 35 cycles of 94 °C for 2 min, 55 °C for 2 min, and 72 °C for 2 min. The resulting 62-mer library contained monothiophosphate substitutions at the phosphate 5′ to every dA residue, in the S_p configuration with the exception of the primer region on the nontemplate strand. Standard phosphoryl PCR amplification was carried out with a mixture of dNTPs (80 μM each) along with the other reagents for 25 cycles of 94 °C for 1 min, 45 °C for 1 min, and 72 °C for 1 min. For the EMSA, 5′-fluorescein-labeled thioaptamers were synthesized using a PCR primer labeled with fluorescein at the 5′-end. We observed incomplete amplification of the thioaptamers resulting in shorter sequences. This is caused by the formation of secondary structures particularly in GC rich regions (*24*). To minimize this formation of secondary structures of the DNA template, we used Betaine solution (1 M, Sigma) and DMSO (5% v/v, Sigma) in the PCR mixture.

Combinatorial Selection of Thioaptamers. Purified RNase H protein was incubated with the previously nitrocellulose-filtered (to exclude sequences that bind to nitrocellulose) PCR-amplified, monothio DNA library in a binding buffer containing 50 mM Tris-HCl, 1.25 mM $MgCl_2$, 25−400 mM KCl, and 10 mM DTT in a total volume of 50 μL for 1 h at ambient temperature, and then passed over nitrocellulose filters. The filters were washed (4 × 1 mL) with binding buffer to remove the unbound and weakly bound DNA. After the washes, thioaptamers bound strongly to the protein are retained on the filter. A 0.5 mL solution of 8 M urea and 2 M KCl was added to elute the thioaptamers bound to the protein. A negative control experiment without the protein was performed simultaneously to monitor any nonspecific

binding of the thiophosphate library to the filter. The eluted DNA was extracted and PCR amplified for use in the next round of selection. The amplified DNA was analyzed by nondenaturing 15% polyacrylamide gel electrophoresis. The stringency of selection was tightened at each selection round by decreasing the amount of protein and by gradually increasing the salt concentration (from 25 to 400 mM) in the binding buffer. A subset of sequences from the initial library and from selection rounds 5, 8, 12, and 14 were determined. A chemically synthesized double stranded 62-mer, 5′-ATAGTTACTAACTGACAGTACACTAGT-GAACTTGATGTTAGACTGAAGTACTTTAACATACC-3′, was used as a control for the inhibition experiments. The sequence of this random 62-mer does not have any transcription factor binding sites. Since NF-κB and AP-1 transcription factor binding sites are found in the promotor region of the HIV-1 LTR (*25*, *26*), ODNs able to bind to these sites would interfere with viral replication. We also tested the effect of an AP-1-specific ODN, XBY-S2. Thioaptamer XBY-S2 (*27*) is a 14-mer with six dithiophosphate substitutions (5′-CCAGTGACTCAGTG-3′) that includes a consensus AP-1 binding site.

Electrophoresis Mobility Shift Assay. One of the selected thioaptamers, R12-2, was used to test the specific binding to RNase H. R12-2 was enzymatically labeled at the 5′-end with fluorescein and was incubated with increasing concentrations of the protein (isolated RNase H domain or intact HIV-1 RT RNase H) in 50 mM Tris-HCl buffer (pH 8), 10 mM $MgCl_2$, and 40 mM DTT at 37 °C for 30 min. The reaction mixture was loaded onto a native 8% polyacrylamide gel, which was electrophoresed and analyzed on a FluorChem 8800 imager (Alpha Innotech). A similar experiment was performed with the *E. coli* RNase H, to test whether R12-2 binds to the RNase H from *E. coli*.

HIV-1 RT RNase H Activity Assay. A DNA−RNA heteroduplex containing radiolabeled RNA was prepared as a substrate for RNase H. A tritium-labeled 18-mer RNA molecule, stem loop 2 of the HIV-1 psi-RNA (*28*), was made by in vitro transcription using T7 RNA polymerase with a mixture of ATP, CTP, GTP, and [^{3}H]UTP. Transcribed RNA was purified by centrifugation using Microcon YM-3 filters (Amicon) to remove unused NTPs and short RNA sequences. The purified RNA was annealed with the complementary DNA strand to form an RNA−DNA hybrid in which the RNA strand was labeled with ^{3}H. HIV-1 RT (0.35 μM) was incubated with the R12-2 thioaptamer (0.5−2.0 μM) in a buffer containing 50 mM Tris-HCl (pH 8.0), 6 mM $MgCl_2$, 10 mM DTT, and 80 mM KCl for 30 min at 37 °C. To this mixture was added the labeled RNA−DNA hybrid (40 000 cpm) to a final volume of 50 μL, and the mixture was incubated at 37 °C for 20 min. The reaction was quenched by the addition of 150 μL of 10% trichloroacetic acid, and the mixture was placed on ice for 10 min. The reaction mixture was filtered and washed, and the amount of radioactivity in the filtrate was measured using a scintillation counter (Beckman Coulter). Radioactivity in the filtrate would be proportional to RNase H activity. A control experiment was performed without any HIV-1 RT, and 100% RNase H activity is assumed in the absence of any R12-2 thioaptamer.

NMR Spectroscopy. Uniformly ^{15}N-labeled RNase H and chemically synthesized R12-2 were used to monitor the binding of the R12-2 thioaptamer to the isolated RNase H domain. The oligonucleotide concentrations were calculated from the absorbance values and the molar absorption coefficients calculated using the nearest neighbor parameters. ^{15}N HSQC spectra (*29*) of the isolated RNase H in the presence of 25 mM $MgCl_2$ were acquired on a Varian UnityPlus 750 MHz instrument equipped with pulse field gradients and triple-resonance probes. One-dimensional proton NMR and 2D NOESY spectra (mixing time of 250 ms) of the R12-2 thioaptamer in a 95% H_2O/5% D_2O mixture were collected. The signals from the R12-2 imino protons, which are very sensitive to changes in the DNA conformation, were monitored during the titration of RNase H to R12-2.

Viruses and Cells. HIV-1 SF162-R5 is a primary isolate that uses CCR5 as a coreceptor, and was obtained from the NIH AIDS Research and Reference Reagent Program. U373-MAGI-CCR5 cells have modifications of the U373 astrocytoma adherent cells that are used for HIV transfection and infection experiments. U373-MAGI-CCR5 cells express β-gal under the control of the HIV LTR, which is transactivated by the HIV Tat protein in relation to the level of virus replication. In addition, these cells express CD4 and the human chemokine receptor CCR5 on its surface, which allow infection by primary HIV-1 strains. U373 cells are propagated in 90% Dulbecco's modified Eagle's medium (DMEM), 10% fetal bovine serum, 0.2 mg/mL G418, 0.1 mg/mL hydromycin B, and 1.0 μg/mL puromycin. For transfection and infection experiments, U373 cells were maintained in 90% DMEM, 10% fetal bovine serum, and 1% penicillin/streptomycin. Thioaptamer R12-2, AP-1-specific XBY-S2, or the random 62-mer ODNs were transfected into the cells 24 h prior to infection using Oligofectamine (OF) liposomes, according to the manufacturer's instructions (Invitrogen).

Infection of ODN-Transfected U373-MAGI-CCR5 Cells. Transfected cells and control cells were infected with HIV-1 at a moi of 0.003 (which consistently gives high levels of viral production) for 2 h. Equal volumes of medium were then added, and the infection was continued for 48 h. HIV-1 replication was quantified in cell lysates by measurement of β-gal activity, as determined by luminometry using the β-Glo kit (Promega) according to the manufacturer's guidelines. β-Gal activity is expressed as relative light units (RLU). To determine the HIV-1 $TCID_{50}$ (50% tissue culture infective dose) in U373-MAGI-CCR5 cells, serial dilutions (10×) of the SF162-R5 virus supernatant were inoculated onto a 24-well plate containing 3×10^4 U373 cells for 2 h, then equal volumes of complete medium were added, and the infection was continued for 48 h. Cells then were lysed and assayed for HIV-directed β-gal expression, and $TCID_{50}$ values were calculated from quadruplicate runs. The p24 antigen concentrations were measured (p24 antigen capture assay, Beckman-Coulter) to determine virus production in culture supernatants harvested at day 7 post-infection.

RESULTS

PCR Amplification of Thioaptamers. For the amplification of DNA sequences with monothiophosphate substitutions, dATP(αS) was used in the PCR mixture (thio-PCR) along with dGTP, dTTP, and dCTP. Only the S_p isomer of the

Round-Clone	Sequence	Length
Class I		
12-3	GGGGTGG--GTGTAC A-GTGGAAGG-	22
12-7	GGGGCGG--GTGTAC A-GTGGAAGG-	22
12-8	GGGGCGG--GTGTAC A-GTGGAAGG-	22
12-14	GGGGTGG--GTGTAC A-GTGGAAGG-	22
12-11	GGGGTGG--GTGTGC A-GTGGAAGG-	22
14-5	GGGGTGG--GTGTGC A-GTGGAAGG-	22
12-9	GGGTTGG--GTGTAC A-GTTGAGGG-	22
12-2	GGGGTTG--GTGTAC A-GTGGATGG-	22
12-4	GGTGTGGCGGTGTGC A-CGCG-----	20
12-5	GGGGTGG--GTGTAC G-GTGGCAGG-	22
12-15	-CGGTTGCGCTGTCG ACGTGGAG---	22
12-13	GGGGTTGTCGTGTCG AGGCGGG----	22
12-10	CCTGTGGGGGTGTAG T-GTAGAG---	22
14-4	---GGGGTGCTGTCC C-GTGGTCTCC	22
14-3	---GGGGTGTTGTCC T-GTGCTCTCC	22
12-6	GGGGCGG---TCTGC GCGTGTCGGC-	22
	GGGGTGGTGGTGTAC AXGTGGAAGGC	Consensus Sequence
Class II		
12-17	CCTGGGGTTGGTGTGTGCAGG	21
12-18	GTGAGCGGCGGGAACACACCG	21
14-10	GGTCGGNNCGGTTNAAGGCC	20
14-6	GGTGTACGGGGAGCACGACGG	21
Class III		
14-13	CGGGNCCG---GCAC AGG----	15
14-15	--TGTGGGGGCCCAG GGG----	16
12-21	-GGGTTGGG--GCG- -------	11
14-16	-GGGTTGGG--GCG- -------	11
14-7	CTGTGTGGG--G--- -------	10
14-8	-GGGTCGGG--GCG- -------	11
14-9	---GT--G---GCGC GGGG---	11
14-11	-GGGTTGGG--GCG- -------	11
14-12	--GGGCTGG--GCG- -----	10

FIGURE 2: Sequences of the selected thioaptamers after the 12th and 14th rounds of selection. Only the variable region of the thioaptamer is shown. Sequences exhibiting higher degrees of alignment are grouped in class I, and those with lower degrees of alignment are in class II. Truncated sequences are listed under class III.

dATP(αS) is used as a substrate by the AmpliTaq DNA Polymerase enzyme to yield the pure R_p stereoisomer (*30*). Yields from the thio-PCR were 20−35% lower compared to yields obtained using all four normal dNTPs. To compensate for the loss of yield in the thio-PCR, reaction conditions were changed by doubling the concentrations of dATP(αS), increasing the annealing temperature by 10 °C from 45 to 55 °C, and increasing the number of PCR cycles from 25 to 35.

Sequences of Selected Thioaptamers. After 12 rounds of selection, the monothio library converged to a few predominant sequences out of the starting library containing (hypothetically) 10^{14} different sequences. Sequences from the variable region of the thioaptamers selected after the 12th and 14th rounds shown in Figure 2 were grouped into three classes based on primary sequence alignment by Clustal W (*31*). Sequences that showed very high degrees of alignment are placed in class I, while those that do not align well are listed under class II. The aptamers with truncated variable regions are listed under class III. These truncated thioaptamers had 10−15 bp in the variable region as opposed to 22 bp in the original library. It is possible that the shorter thioaptamers (class III) could have been formed by inefficient or incomplete amplification of the library during the PCR cycles. However, sequences in all three classes showed similar sequence motifs. The sequences of the selected thioaptamers showed G-rich sequences at their 5′-ends. These G rich sequences, with a minimum of four interspersed G nucleotides, are known to have the potential to form G-quartet structures (*32*−*34*). Recent reports of single-strand DNA aptamers selected against HIV-1 RT, HIV-1 integrase, and human RNase H also showed G-rich sequences that could form G-quartet structures (*16*−*18*, *35*).

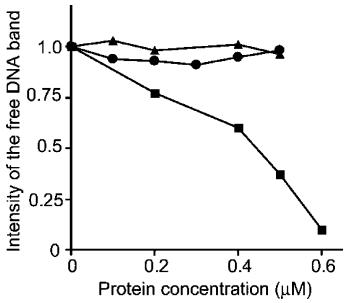

FIGURE 3: Binding of thioaptamer R12-2 to different proteins. EMSA of R12-2 shows binding to the RNase H domain of HIV-1 RT (■) but not to the *E. coli* RNase H (●). The initial library clone (▲) did not show binding to the HIV-1 RT. The intensity of the free DNA band is plotted against the protein concentration.

EMSAs Exhibited Selective Binding of R12-2 to the RNase H Domain of HIV-1 RT. In EMSA experiments, the lead thioaptamer R12-2 exhibited specific binding to the isolated RNase H domain of HIV-1 RT (Figure 3). The intensity of the free DNA band (lower band) decreased with an increase in RNase H concentration, showing the enhanced binding of R12-2 with the increase in protein concentration. Under identical conditions, however, the R12-2 did not show any significant binding to the RNase H of *E. coli*, a structurally similar protein. Similarly, the initial library did not show

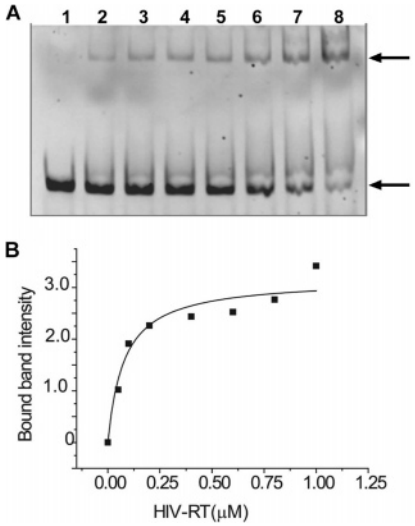

FIGURE 4: EMSA of binding of lead thioaptamer R12-2 to HIV-1 RT. (A) Gel electrophoresis mobility shift assay showing binding of R12-2 to the HIV-1 RT. The arrows show the positions of upper and lower bands: lane 1, no protein; and lanes 2−8, proteins at increasing concentrations (0.05, 0.1, 0.2, 0.4, 0.6, 0.8, and 1 μM, respectively). (B) Quantitative measurement of the intensity of the DNA band bound to the protein. The intensity of the upper band is plotted against the HIV RT concentration in micromolar (the bound band intensities are blanked against the intensity of the band at the HIV RT concentration of 0.0).

any binding to the isolated RNase H domain of HIV-1 RT or to the intact HIV-1 RT (Figure 3). We also tested the binding of R12-2 to the intact HIV-1 RT. Two bands were visible in these gels (Figure 4A). The lower band corresponds to the free oligonucleotide, and the shifted upper band corresponds to the oligonucleotide bound to the protein. The presence of protein in the upper band was detected by staining the gel with Coomassie blue. With increasing protein concentrations, the intensity of the protein-bound DNA band (upper band) increased while the intensity of the free DNA band (lower band) decreased. This observation shows that R12-2 is binding to the HIV-1 RT. The quantitative binding of R12-2 to the HIV-1 RT is shown in the plot of bound band intensity versus protein concentration (Figure 4B). The dissociation constant (K_d), determined from nonlinear regression analysis with the Hill plot method using Origin, was 70 nM.

NMR Spectroscopy Showed R12-2 Interacts with the RNase H Domain of HIV-1 RT. We used NMR spectroscopic methods to demonstrate the binding of R12-2 to the isolated RNase H domain (data not shown). Imino proton signals of R12-2, the most sensitive indicators of the structural perturbations in DNA conformation, showed broadening with the addition of RNase H, indicating the binding of R12-2 to the protein. The line widths of the imino proton signals increased with the increase in protein concentration, and these signals eventually disappeared.

Inhibition of RNase H Activity by Thioaptamer R12-2. The ability of R12-2 to inhibit the RNase H activity was tested using a radiolabeled RNA−DNA hybrid duplex, as described in Materials and Methods. Although the RNase H domain can be expressed and isolated as a stable protein, the isolated protein is inactive or very weakly active (*23*, *36*, *37*). Therefore, for the inhibition assay (Figure 5), we used the intact HIV-1 RT instead of the isolated RNase H domain.

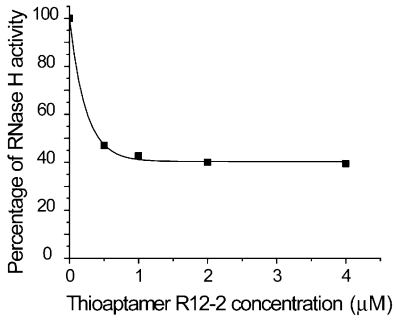

FIGURE 5: Effect of selected aptamer R12-2 on the RNase H activity of HIV-1 RT. Radioactivity retained in the filtrate, considered as a measure of RNase H activity, is plotted against the thioaptamer concentration.

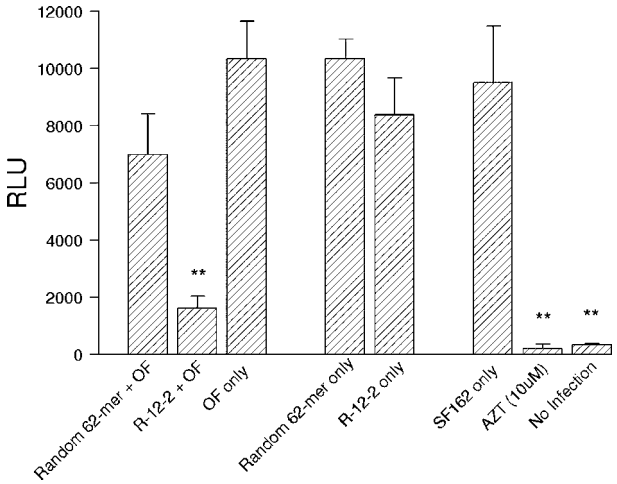

FIGURE 6: Effect of R12-2 on cell infection. U373-R5 indicator cells were transfected with R12-2 or random 62-mer and then infected the next day with the SF-162 virus strain. Viral replication was assessed after 48 h by measuring β-gal activity in cell lysates by luminometry. Controls include mock transfected cells (OF only), thioaptamers without the transfection reagent, and 10 μM AZT at the time of infection. Significant differences compared to the mock transfected controls are denoted with asterisks.

The assay was based on the ability of the RNase H catalytic function in intact HIV-1 RT to cleave the RNA strand in the RNA−DNA heteroduplex. Addition of 0.5 μM R12-2 decreased the RNase H activity to 47% compared to the control, where no R12-2 was present. Additional R12-2 decreased the RNase H activity further to 39%. However, when the R12-2 concentration was increased higher than 2 μM, no further reduction in RNase H activity was observed.

R12-2 Exhibited Dose-Dependent Inhibition of HIV-1 Replication in Vitro. Incubation of U373-MAGI-CCR5 cells, which had been transfected with Oligofectamine (OF) and thioaptamer R12-2 24 h prior to infection with HIV-SF162-R5 (2 ng, at a moi of 0.003), a prototypic primary HIV strain, resulted in a significant reduction in the level of infection, as compared to the cells transfected with the random 62-mer (Figure 6). Inhibition of the HIV-1 infection by AZT is shown for comparison. The ODN specific to the human AP-1, XBY-S2, also showed modest effects on HIV infection (Figure 7). However, the inhibition by the R12-2 is significantly stronger than the inhibition by XBY-S2. The sequence of XBY-S2 includes a consensus AP-1 binding site, and would influence the expression of immune responses in the cell by sequestering AP-1 proteins. The modest inhibition exhibited by XBY-S2 may be due to its ability to serve as a

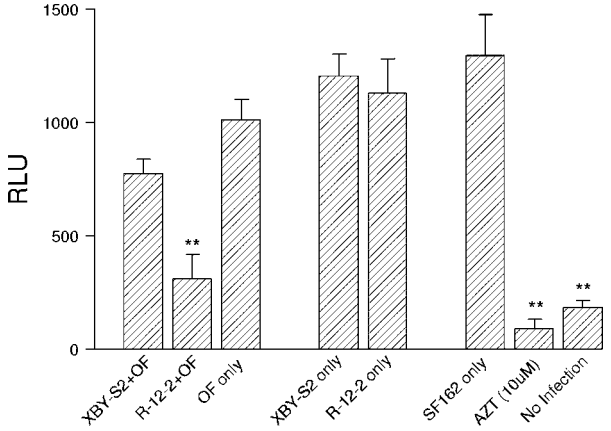

FIGURE 7: Comparison of inhibition by thioaptamers R12-2 and XBY-S2. Viral replication was determined after 48 h by measuring β-gal activity in cell lysates by luminometry. Controls include mock transfected cells (OF only), thioaptamers without the transfection reagent, and 10 μM AZT at the time of infection.

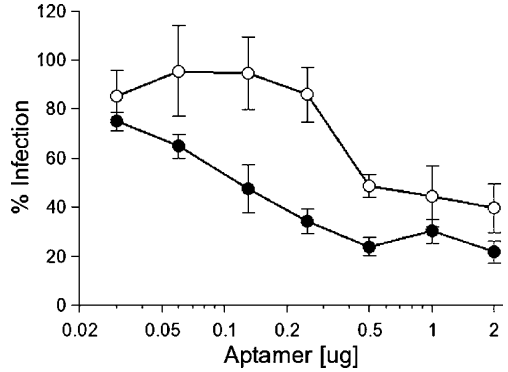

FIGURE 8: Dose response after treatment with thioaptamers R12-2 (●) and XBY-S2 (○). Indicator U373-MAGI-CCR5 cells were transfected with various doses of thioaptamer 24 h prior to infection with HIV SF162, and analyzed for β-gal activity (RLU) after 48 h. Results are presented as the percentage of virus production compared with untreated controls.

decoy to bind to AP-1 transcription factors. A dose-dependent inhibitory response was demonstrated, with R12-2 doses ranging from 0.03 to 2.0 μg/mL (IC_{50} < 100 nM) to the same low level as 10 μM AZT (Figure 8). However, the AP-1-specific thioaptamer XBY-S2 did not show a significant change in inhibition up to the dose level of 0.25 μg/mL. At higher concentrations (>0.5 μg/mL), both XBY-S2 and R12-2 did not exhibit significant change in the percentage of inhibition. Transfection of R12-2 (0.05 μg/mL) resulted in the inhibition of viral replication across a broad range of HIV-SF162-R5 inocula ranging from a moi of 0.0005 (0.3 ng) to 0.05 (30 ng) as shown in Figure 9. R12-2 showed significant inhibition of the virus at high moi values, and viral replication is comparable to that seen with AZT when the moi ≤ 0.005 (0.3 ng of p24 as measured by the p24 antigen capture ELISA method). R12-2 does not show any cytotoxicity to the cells (data not shown).

DISCUSSION

ODNs are emerging as promising alternative therapeutic agents. However, to increase the resistance to digestion by cellular enzymes, modified ODNs have to be developed. Modifications in the phosphate backbone will significantly affect their binding to target proteins, because most of the

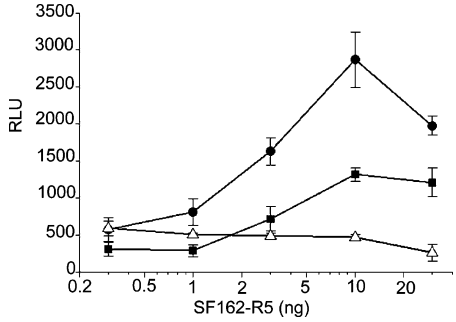

FIGURE 9: Effect of thioaptamer R12-2 with increasing virus inocula. Two-fold dilutions of the SF162 supernatant were used to infect U373-MAGI-CCR5 cells 24 h after thioaptamer transfection or control condition, and infection was quantified in cell lysates after 48 h (RLU). Filled circles (●) represent data for untransfected cells, filled squares (■) those for cells transfected with R12-2, and empty triangles (△) those for control AZT (10 μM).

direct contacts between DNA-binding proteins and their binding sites in DNA involved the phosphate groups (*38*, *39*). Sulfur substitutions of the phosphoryl oxygens of ODNs often lead to their enhanced binding to numerous proteins (*21*, *22*). However, complete substitution of phosphoryl oxygens with sulfur appears to make thioaptamers too "sticky" such that they lose their ability to discriminate between target and nontarget proteins. Therefore, the total number and positions of thio-substituted phosphates have to be optimized using either rational design principles or combinatorial techniques to decrease the level of nonspecific protein binding, and to enhance only the specific favorable interactions with proteins such as RNase H. Phosphorothioate modifications show increased resistance to digestion by cellular nucleases and often have a higher affinity for binding to proteins. They can also be readily synthesized in high yields and enhance favorable pharmacokinetic properties (*40*). Various pharmacokinetic studies in animals have shown that phosphorothioate analogues are rapidly dispersed to various tissues and cleared through the kidney within acceptable time periods (*41*). By using only the dATP(αS) during PCR amplification cycles, we have produced thioaptamers that have thio substitutions only at positions 5′ to the dA residues. Combinatorial selection methods that allow screening of a large number of random sequences in nucleic acid libraries for affinity to proteins facilitate the selection of ODNs that would have the optimal number of thiophosphate substitutions. Our lead thioaptamer, R12-2, exhibited selective binding to the RNase H of HIV-1 RT. This thioaptamer did not bind to the *E. coli* RNase H, even though these two proteins are structurally similar. By using selection methods and combinatorial synthesis which incorporates selective sulfur substitution, we have selected a DNA thioaptamer that binds tightly and specifically to the RNase H domain of HIV-1 RT, inhibits the RNase H activity in vitro, and inhibits HIV-1 replication in cell cultures. The selected thioaptamer did not bind to the *E. coli* RNase H, a structurally similar protein.

Although the RNase H domain of the HIV-1 RT can be expressed and isolated as a stable protein, the isolated domain is either catalytically inactive or very weakly active. This loss of catalytic activity in the isolated domain is probably not caused by structural differences between the two forms, because the RNase H structures in isolation and in the intact RT are very similar (*42*, *43*). The basis for the inactivity of

the isolated domain is attributed mainly to the increased dynamics. Recent NMR studies on the backbone dynamics of the isolated RNase H domain indicate that the intramolecular dynamic behavior of the isolated domain is severe, resulting in the loss of catalytic activity of RNase H in isolation (*44*, *45*). Since we have used the isolated RNase H domain in our iterative selection rounds, the selected thioaptamers are presumed to specifically bind to the RNase H domain of intact RT. However, R12-2 is a 62-mer duplex, and other regions of the duplex very likely extend into the polymerase site of the RT, as observed in various duplex DNA−RT X-ray crystal structures and models (*46*, *47*). R12-2 reduced the RNase H activity of RT by 50%. However, the inhibition of viral production was more dramatic (Figure 6). It is quite possible that the difference in the inhibition levels between the RNase H activity and the viral production could be the result of R12-2's inhibition of the polymerase activity of RT. The selected thioaptamer, R12-2, inhibits the function of the RNase H in the intact HIV-1 RT. Because the structures of the RNase H domain are similar in isolation and in intact HIV-1 RT, selecting thioaptamers against the isolated domain that could inhibit the function of the intact HIV-1 RT would be a better choice than selecting aptamers against the intact HIV-1 RT. Selecting against intact HIV-1 RT does not guarantee that the selected aptamer will bind to the RNase H domain. In fact, the selected aptamer may bind to the polymerase domain rather than to the RNase H domain. Perhaps sequences selected against the RNase H domain and intact HIV-1 RT could be used adjunctively. As far as we are aware, this is the first report of an aptamer that was selected to target the isolated domain of RNase H.

R12-2 exhibited significant, dose-dependent inhibition of HIV-1 infection. AP-1-specific thioaptamer XBY-S2 also showed modest inhibition of infection at higher aptamer concentrations ($>0.5\ \mu$g/mL). The XBY-S2 thioaptamer was found to bind AP-1 proteins from a macrophage-like cell line, and inhibits the binding of the AP-1 transcription factor to DNA (D. G. Gorenstein, personal communication). An AP-1 binding site is shown to be present in the promoter region of the HIV-1 LTR (*25*). The modest inhibition of HIV-1 infection by XBY-S2 might be due to its ability to bind to AP-1. Inhibition by R12-2 was seen across a broad range of HIV inocula, and it was comparable to AZT treatment at a low moi. The inhibition at a high moi is noteworthy, since transfection efficiency ("uptake") of the virus or thioaptamer in some experiments was only 80%. Thus, the thioaptamer activity may be underestimated when compared with the activity of drugs, such as AZT, which are taken up by essentially every viable cell in the culture.

As the HIV epidemic continues to mature through treatment error and emerging resistance to the initial classes of antiretroviral drugs, which include the HIV-1 RT inhibitors, there will be a need to develop treatments directed to new targets. The various inhibitors of HIV entry, targeting attachment, coreceptor binding, and fusion will have a substantial impact on the ability to suppress viremia as they are developed for clinical use by extending treatment options, but additional new classes of drug will inevitably be needed. Combinatorial selection of thioaptamers that bind to novel targets may allow development of therapeutic agents directed to diverse viral functions.

ACKNOWLEDGMENT

We thank Dr. R. Hodge and the NIEHS synthetic core facility at the University of Texas Medical Branch for the chemical synthesis of DNAs, Dr. X. Yang for providing the XBY-S2 sample, and Drs. N. Herzog, D. Kallick, and D. Volk for helpful discussions.

REFERENCES

1. Schatz, O., Mous, J., and Le Grice, S. F. J. (1990) HIV-1 RT-associated ribonuclease H displays both endonuclease and 3′−5′ exonuclease activity, *EMBO J. 9*, 1171−1176.
2. Palella, F. J., Jr., Delaney, K. M., Moorman, A. C., Loveless, M. O., Fuhrer, J., Satten, G. A., Aschman, D J., and Holmberg, S. D. (1998) Declining morbidity and mortality among patients with advanced human immunodeficiency virus infection. HIV Outpatient Study Investigators, *N. Engl. J. Med. 338*, 853−860.
3. Yeni, P. G., Hammer, S. M., Hirsch, M. S., Saag, M. S., Schechter, M., Carpenter, C. C., Fischl, M. A., Gatell, J. M., Gazzard, B. G., Jacobsen, D. M., Katzenstein, D. A., Montaner, J. S., Richman, D. D., Schooley, R. T., Thompson, M. A., Vella, S., and Volberding, P. A. (2004) Treatment for adult HIV infection: 2004 recommendations of the International AIDS Society-USA Panel, *J. Am. Med. Assoc. 292*, 251−265.
4. Hirsch, M. S., Brun-Vezinet, F., Clotet, B., Conway, B., Kuritzkes, D. R., D'Aquila, R. T., Demeter, L. M., Hammer, S. M., Johnson, V. A., Loveday, C., Mellors, J. W., Jacobsen, D. M., and Richman, D. D. (2003) Antiretroviral drug resistance testing in adults infected with human immunodeficiency virus type 1: 2003 recommendations of an International AIDS Society-USA Panel, *Clin. Infect. Dis. 37*, 113−128.
5. Ferguson, M. R., Rojo, D. R., von Lindern, J. J., and O'Brien, W. A. (2002) HIV-1 replication cycle, *Clin. Lab. Med. 3*, 611−635.
6. Majumdar, C., Stein, C. A., Cohen, J. S., Broder, S., and Wilson, S. H. (1989) Stepwise mechanism of HIV reverse transcriptase: Primer function of phosphorothioate oligodeoxynucleotide, *Biochemistry 28*, 1340−1346.
7. Tuerk, C., MacDougal, S., and Gold, L. (1992) RNA pseudoknots that inhibit human immunodeficiency virus type 1 reverse transcriptase, *Proc. Natl. Acad. Sci. U.S.A. 89*, 6988−6992.
8. Stein, C. A., and Cheng, Y. C. (1993) Antisense oligonucleotides as therapeutic agents: Is the bullet really magical? *Science 261*, 1004−1012.
9. Morgan, R. A., and Walker, R. (1996) Gene therapy for AIDS using retroviral mediated gene transfer to deliver HIV-1 antisense TAR and transdominant Rev protein genes to syngeneic lymphocytes in HIV-1 infected identical twins, *Hum. Gene Ther. 7*, 1281−1306.
10. Ellington, A. D., and Szosytak, J. W. (1990) In vitro selection of RNA molecules that bind specific ligands, *Nature 346*, 818−822.
11. Gold, L., Polisky, B., Uhlenbeck, O. C., and Yarus, M. (1995) Diversity of oligonucleotide functions, *Annu. Rev. Biochem. 64*, 763−797.
12. King, D. J., Bassett, S. E., Li, X., Fennewald, S. A., Herzog, N. K., Luxon, B. A., Shope, R., and Gorenstein, D. G. (2002) Combinatorial selection and binding of phosphorothioate aptamers targeting human NF-κB RelA(p65) and p50, *Biochemistry 41*, 9696−9706.
13. Agarwal, S. (1991) Antisense oligonucleotides: Possible approaches for the chemotherapy of AIDS, in *Prospects for antisense nucleic acid therapy of cancer and AIDS* (Wickstrom, E., Ed.) pp 143−159, Liss, New York.
14. Schneider, D. J., Feigon, J., Hostomsky, Z., and Gold, L. (1995) High-affinity ssDNA inhibitors of the reverse transcriptase of type 1 human immunodeficiency virus, *Biochemistry 34*, 9599−9610.
15. Nickens, D. G., Patterson, J. T., and Burke, D. H. (2003) Inhibition of HIV-1 reverse transcriptase by RNA aptamers in *Escherichia coli*, *RNA 9*, 1029−1033.
16. Andreola, M. L., Pileur, F., Calmels, C., Ventura, M., Tarrago-Litvak, L., Toulme, J. J., and Litvak, S. (2001) DNA aptamers selected against the HIV-1 RNase H display in vitro antiviral activity, *Biochemistry 40*, 10087−10094.
17. Pileur, F., Andreola, M. L., Dausse, E., Michel, J., Moreau, S., Yamada, H., Gaidamakov, S. A., Crouch, R. J., Toulme, J. J., and Cazenave, C. (2003) Selective inhibitory DNA aptamers of the human RNase H1, *Nucleic Acids Res. 31*, 5776−5788.

18. de Solutrait, V. R., Lozach, P., Altmeyer, R., Tarrago-Litvak, L., Litvak, S., and Andreola, M. L. (2002) DNA aptamers derived from HIV-1 RNase H inhibitors are strong anti-integrase agents, *J. Mol. Biol. 324*, 195−203.
19. Paoletti, A. C., Shubsda, M. F., Hudson, B. S., and Borer, P. N. (2002) Affinities of the nucleocapsid protein for variants of SL3 RNA in HIV-1, *Biochemistry 41*, 15423−15428.
20. Shubsda, M. F., Paoletti, A. C., Hudson, B. S., and Borer, P. N. (2002**)** Affinities of packaging domain loops in HIV-1 RNA for the nucleocapsid protein, *Biochemistry 41*, 5276−5282.
21. Milligan, J. F., and Uhlenbeck, O. C. (1989) Determination of RNA-protein contacts using thiophosphate substitutions, *Biochemistry 28*, 2849−2855.
22. Marshall, W. S., and Caruthers, M. H. (1993) Phosphorodithioate DNA as a potential therapeutic drug, *Science 259*, 1564−1570.
23. Becerra, S. P., Clore, G. M., Gronenborn, A. M., Karlstrom, A. R., Stahl, S. J., Wilson, S. H., and Wingfield, P. T. (1990) Purification and characterization of the RNase H domain of HIV-1 reverse transcriptase expressed in recombinant *Escherichia coli*, *FEBS Lett. 270*, 76−80.
24. Henke, W., Herdel, K., Jung, K., Schnorr, D., and Loening, S. A. (1997) Betaine improves the PCR amplification of GC-rich DNA sequences, *Nucleic Acids Res. 25*, 3957−3958.
25. Liou, H. C., and Baltimore, D. (1993) Regulation of the NF-κB/rel transcription factor and I κB Inhibitor System, *Curr. Opin. Cell Biol. 5*, 477−487.
26. Nabel, G., and Baltimore, D. (1987) An inducible transcription factor activates expression of human immunodeficiency virus T cells, *Nature 326*, 711−713.
27. Yang, X., and Gorenstein, D. G. (2004) Progress in thioaptamer development, *Curr. Drug Targets 5*, 705−715.
28. Amarasinghe, G. K., De Guzman, R. N., Turner, R. B., Chancellor, K. J., Wu, Z. R., and Summers, M. F. (2000) NMR structure of the HIV-1 nucleocapsid protein bound to stem-loop SL2 of the ψ-RNA packaging signal. Implications for genome recognition, *J. Mol. Biol. 301*, 491−511.
29. Bax, A., and Pochapsky, S. S. (1992) Optimized recording of heteronuclear multidimensional NMR spectra using pulsed field gradients, *J. Magn. Reson. 99*, 638−643.
30. Eckstein, F., and Thomson, J. B. (1995) Phosphate analogs for study of DNA polymerases, *Methods Enzymol. 262*, 189−202.
31. Thompson, J. D., Higgins, D. G., and Gibson, T. J. (1994) CLUSTAL W: Improving the sensitivity of progressive multiple sequence alignment through sequence weighting, position-specific gap penalties and weight matrix choice, *Nucleic Acids Res. 22*, 4673−4680.
32. Williamson, J. R., Raguraman, M. K., and Cech, T. R. (1989) Monovalent cation-induced structure of telomeric DNA: The G-quartet model, *Cell 59*, 871−880.
33. Smith, F. W., and Feigon, J. (1992) Quadruplex structure of *Oxytricha* telomeric DNA oligonucleotides, *Nature 356*, 164−168.
34. Bianchi, A., and de Lange, T. (1999) Ku binds telomeric DNA in vitro, *J. Biol. Chem. 274*, 21223−21227.
35. Phan, A. T., Kuryavyi, V., Ma, J. B., Faure, A., Andreola, M. L., and Patel, D. J. (2005) An interlocked dimeric parallel-stranded DNA quadruplex: A potent inhibitor of HIV-1 integrase, *Proc. Natl. Acad. Sci. U.S.A. 102*, 634−639.
36. Evans, D. B., Brawn, K., Deibel, M. R., Jr., Tarpley, W. G., and Sharma, S. K. (1991) A recombinant ribonuclease H domain of HIV-1 reverse transcriptase that is enzymatically active, *J. Biol. Chem. 266*, 20583−20585.
37. Hostomsky, Z., Hostomska, Z., Hudson, G. O., Moomaw, E. W., and Nodes, B. R. (1991) Reconstitution in vitro of RNase H activity by using purified N-terminal and C-terminal domains of human immunodeficiency virus type 1 reverse transcriptase, *Proc. Natl. Acad. Sci. U.S.A. 88*, 1148−1152.
38. Botuyan, M. V., Keire, D. A., Kroen, C., and Gorenstein, D. G. (1993) ^{31}P nuclear magnetic resonance spectra and dissociation constants of lac repressor headpiece·duplex operator complexes: The importance of phosphate backbone flexibility in protein·DNA recognition, *Biochemistry 32*, 6863−6874.
39. Cho, Y., Zhu, F. C., Luxon, B. A., and Gorenstein, D. G. (1993) 2D ^{1}H and ^{31}P NMR spectra and distorted A-DNA-like duplex structure of a phosphorodithioate oligonucleotide, *J. Biomol. Struct. Dyn. 11*, 685−702.
40. Tonkinson, J. L., Guvakova, M., Khaled, Z., Lee, J., Yakubov, L., Marshall, W. S., Caruthers, M. H., and Stein, C. A. (1994) Cellular pharmacology and protein binding of phosphoromonothioate and phosphorodithioate oligodeoxynucleotides: A comparative study, *Antisense Res. Dev. 4*, 269−278.
41. Gallo, M., Montserrat, J. M., and Iribarren, A. M. (2003) Design and applications of modified oligonucleotides, *Braz. J. Med. Biol. Res. 36*, 143−151.
42. Davies, J. F., Hostomska, Z., Hostomsky, Z., Jordan, S. R., and Matthews, D. A. (1991) Crystal structure of the ribonuclease H domain of HIV-1 reverse transcriptase, *Science 252*, 88−95.
43. Chattopadhyay, D., Finzel, B. C., Munson, S. H., Evans, D. B., Sharma, S. K., Strakalaitis, N. A., Brunner, D. P., Eckenrode, F. M., Dauter, Z., Betzel, C., and Einspahr, H. M. (1993) Crystallographic analyses of an active HIV-1 ribonuclease H domain show structural features that distinguish it from the inactive form, *Acta Crystallogr. 49*, 423−427.
44. Pari, K., Mueller, G. A., DeRose, E. F., Kirby, T. W., and London, R. E. (2003) Solution structure of the RNase H domain of the HIV-1 reverse transcriptase in the presence of magnesium, *Biochemistry 42*, 639−650.
45. Mueller, G. A., Pari, K., DeRose, E. F., Kirby, T. W., and London, R. E. (2004) Backbone dynamics of the RNase H domain of HIV-1 reverse transcriptase, *Biochemistry 43*, 9332−9342.
46. Jacobo-Molina, A., Ding, J., Nanni, R. G., Clark, A. D., Lu, X., Tantillo, C., Williams, R. L., Kamer, G., Ferris, A. L., Clark, P., Hizi, A., Hughes, S. H., and Arnold, E. (1993) Crystal structure of human immunodeficiency virus type 1 reverse transcriptase complexed with double-stranded DNA at 3.0 Å resolution shows bent DNA, *Proc. Natl. Acad. Sci. U.S.A. 90*, 6320−6324.
47. Bebenek, K., Berad, W. A., Darden, T. A., Prasad, R., Luxon, B. A., Gorenstein, D. G., Wilson, S. M., and Kunkel, T. A. (1997) A minor groove binding track in reverse transcriptase, *Nat. Struct. Biol. 4*, 194−197.

BI0507074